SUPERCONDUCTOR DESIGN AND LOSS ANALYSIS FOR A 20 MJ INDUCTION HEATING COIL*

M. S. Walker, J. G. Declercq, B. A. Zeitlin, J. D. Scudiere, and M. J. Ross, Intermagnetics General Corporation;
M. A. Janocko, S. K. Singh, E. A. Ibrahim, and P. W. Eckels, Westinghouse Electric Corporation;
and J. D. Rogers and J. J. Wollan, Los Alamos Scientific Laboratory

SUMMARY

The design of a 50 kAmpere conductor for use in a 20 MJ Induction Heating Coil is described. The conductor is a wide flat cable of 36 subcables, each of which contains six Nb-Ti strands around a stainless steel core strand. It is cryostable, with a pool-boiling, fully-normal equivalent heat transfer from the unoccluded strand surface of 0.26 Watts/cm^2. A thin, tough polyester amide-imide insulation enhances heat transfer and prevents interstrand coupling. The tightly-twisted strands are configured using Cu-Ni elements to provide low AC losses with Nb-Ti filaments in an all-copper matrix. AC losses are expected to be approximately: (1) 0.3% of 20 MJ for a -7.5 T to 7.5 T one-second 1/2-cosinusoidal bipolar operation in a 20 MJ coil, and (2) for additional reference, 0.1% of 100 MJ for a 1.8 second -8 T to +8 T ramped operation in a 100 MJ coil with a heat transfer of 0.36 Watts/cm^2. The design is based on the manufacture and testing of prototype strands and subcables.

I. INTRODUCTION

The 20 MJ coil design[1] was developed to demonstrate the feasibility of superconducting poloidal systems for Tokamak reactors, to provide confidence in the application of superconductivity to actual reactors, and to provide the opportunity to solve specific engineering problems to support the fusion pulsed coil program. A fundamental part of the design was the choice of conductor concept and conductor design and analysis, including the analysis of conductor losses and stability. This paper presents the conductor design and supporting analyses, with reference to related design choices and prototype conductor strand and cable development and testing.

II. WESTINGHOUSE/IGC APPROACH

It was specified by LASL that the conductor should be designed for cryostable operation through as many as 10^5 cycles of 1/2 cosinusoidal peak field change of -7.5 T to +7.5 T in one second or the return, one of the more demanding of possible conditions anticipated for a TNS or ETF device. Total losses from all sources within the coil operating as a part of a long coil stack are to be less than 0.3% of 20 MJ for a one-second bipolar pulse, or for copper matrix strands <0.3% for a two-second pulse.

To maximize the flux produced by the OH coil for given winding cost and losses, a high current density winding is desirable. However, the conductor must include stabilizer and be subdivided into small elements to reduce the AC losses and to crease surface for heat transfer to meet the specification of cryostability. Sufficient winding stiffness must be retained to prevent losses due to mechanical hysteresis, and the coil must be self-supported with a low loss structure. The achievable current density is, therefore, reduced; and the design is a compromise between the drive for high current density and stability, loss, and structural requirements.

The Westinghouse/IGC approach has been to provide a magnet system that exhibits the long lifetime and integrity normally associated with equipment for the electrical utility industry. A pancake-wound coil approach has been chosen, utilizing primarily G-10 structural materials to support axial loads. The choice of heat transfer for stability is conservative, although the choice of less margin in stability would reduce the required conductor volume and thus lower AC losses. While losses are at manageable and acceptable levels, possible lower-loss designs were rejected in favor of ruggedness and reliability in manufacturing and performance.

*Supported by the University of California, Los Alamos Scientific Laboratory Contract No. 4-XP9-3459H-1.

III. CONDUCTOR DESIGN

The 20 MJ conductor is shown in Figure 1. To maximize winding current density, the steel required for support of the hoop stress is enclosed as a thin high strength (Nitronic 40) core strap of a cable of subcables. The number of subcables was set at 36, within the number accommodated by large conventional cabling machinery. The dimensions of the cable result from a selection of the smallest subcable strands possible, within the constraint that the operating current of 50,000 Amperes be achieved with the assurance of recovery from a fully-normalized long section of conductor. Each subcable consists of six polyester amide-imide (Westinghouse Omega) film-insulated monolithic superconductor strands cabled around a similarly-insulated stainless steel core strand. A description of operating characteristics, component material, parameters and dimensions of the cable is provided in Table 1.

The design of the superconductor strands proceeded through an interactive process consisting of (1) prototype strand design and manufacture, (2) initial 20 MJ strand design, (3) final sizing of the prototype strands to represent very closely the 20 MJ design, (4) test of the prototype strands[2], (5) variation of prototype strand twist pitch length and retest as strand and subcable[2], and (6) alteration of the 20 MJ strand design to incorporate the test results. As a consequence, the 20 MJ strand design is based on the direct measurement of strand parameters for prototype conductors of the 20 MJ design size and of the 20 MJ design configuration.

The Nb-Ti cross section was established on the basis of critical current density measured in Prototype #1 and the choice of 0.71 for I_{op}/I_c margin. The strand configuration was selected as part of a trade-off study that evaluated lower loss solder-together cabled strands of smaller substrands[3] and mixed matrix monolithic strands[4] with copper-nickel webs separating copper-sleeved filaments. The selected design combines the most efficient use of space for superconductor and stabilizer with the avoidance of solder, which would prevent the use of reliable thin, strong cured insulation. The thin copper-nickel ring and fins reduce eddy current losses in and coupling currents through the copper outer sheath, bringing the loss within the target specification for the copper matrix design.

Although no credible event capable of normalizing the cable was identified, the cable was designed to recover from normalization of an entire turn. The final strand size was therefore adjusted to provide a fully-normal heat flux of 0.26 Watts/cm^2 from the unoccluded strand surface, assumed to be 2/3 of the total strand surface. For this calculation, magnetoresistance was estimated from a zero field residual resistivity ratio of 90 (273 K/2.4 K) for the core matrix copper surrounding the filaments and 125 for the remainder of the copper. These values are based upon experimental test results on the prototype strands of high purity OFHC copper having initial RRR greater than 150. Values of resistivity at 4.5 K, 7.5 T of 4.9 x 10^{-8} Ω-cm and 4.7 x 10^{-8} Ω-cm were calculated for the two regions. The electrical conduction of the strands was found in tests on Prototype #2 to be essentially unchanged with twist to the degree specified in this design, while AC losses were substantially reduced[2]. The 2 mm diameter strand

0018-9464/81/0100-0908$00.75 © 1981 IEEE

provides interstitial spaces and channels between crossing strands in adjacent subcables that should be large enough to clear bubbles, based upon (1) the operation of the 540 kiloJoule coil which required passages of this approximate size[5] and (2) observations of boiling helium. The adequacy of bubble clearing will be tested in the 50 kAmp prototype coil. While it is desirable to make the insulation thin and of high thermal conductivity to prevent excessive temperature rise within the strand during recovery and even enhance heat transfer, it should adhere well enough so as not to flake or loosely cover strand surfaces and interfere with helium movement and heat transfer even after 10^5 pulse cycles. Polyester amide-imide insulation has been identified as tough and strongly adhering[6] and tests of this insulation in thin coatings on the prototype strands have confirmed that it provides an adequate toughness and adherence for the low voltage electrical insulation needs of this design[2].

To avoid coupling between the central strand and the outside strands, which would result in large self-field losses for the cable and uneven currnet distribution, the central strand of the subcable is inactive, insulated and of relatively high resistivity to reduce eddy current losses. The insulation scheme for the stainless mandrel was selected on the basis of Westinghouse experience on the 540 kiloJoule and 400 kiloJoule METS coils. A b-stage epoxy-filled fiberglass tape is first wrapped around the mandrel, butt-lapped turn-to-turn, followed by a thin layer of Kapton wrapped over the seams in the epoxy fiberglass, butt-lapped, followed by a second layer of Kapton, butt-lapped to cover the seams in the prior Kapton layer. The design width of the insulated mandrel, w, and pitch angle θ have been determined on the basis of IGC experience with cables and approximate analyses[1]. The cable will be made by cabling all 36 subcables with the same sense of rotation as in the subcables through appropriate spider dies and feeding guides with a final in-line draw through a set of rollers which compacts the cable to the required flat shape, deforming the subcables at the cable edges to provide a set that maintains the cable shape. There will be considerable springback even after this compaction; the dimensions shown in Table 1 are therefore for the cable as tightly wound and axially and radially compressed in the winding, with the springback thus entirely removed. (The fabricability of this design has since been confirmed through the manufacture of the 50 kAmp prototype cable[7]. The pitch angle achieved for the design width is 22°.)

IV. AC LOSSES FOR THE 20 MJ COIL

The operating losses for the coil can arise from two sources: (1) AC losses generated in the metallic components of the winding, and (2) mechanical hysteresis losses resulting from frictional and otherwise inelastic movement within the coil. The mechanical losses are not readily calculable and will eventually be determined by deduction from the measurement of losses during operation of the 20 MJ coil. However, the elements of the cable have been made as large as possible, in part to provide a stiff and tight winding to limit these losses as much as possible while adhering to the remainder of the program specifications.

The central section of the TNS Ohmic heating coil experiences a magnetic field environment approximating that of an infinitely long solenoid. Calculations for comparison with the 20 MJ coil specifications have therefore been performed in this approximation, where radial and azimuthal components of magnetic field change are zero. For comparison with anticipated test results, AC losses have also been calculated for the coil operating alone with the same one-second -50 kAmp to +50 kAmp pulse. The central field is still approximately 7.5 T. The formulae used to calculate the various components of the loss and the losses calculated for both modes of coil operation are shown in Table 2. The distribution of total losses versus coil radius for these two cases in shown in Figure 2. The losses summarized in the Table can be divided into two classes, (1) the hysteretic losses which are independent of bipolar pulse time, and (2) eddy current and coupling losses which are inversely proportional to the pulse time. Generally, true hysteretic losses are independent of pulse time, and for the pulse times considered here, the fully-coupled parallel field loss is hysteretic. The eddy current and coupling losses which comprise over 60% of the losses shown are inversely proportional to pulse time, and accordingly can be substantially reduced for longer pulse times. Although the primary objective of 0.3% loss for the coil operating in a stack for a one-second pulse is marginally exceeded, the calculated 0.26% loss for a two-second pulse meets the alternate program objective for copper matrix conductors. Note that the loss levels shown pertain specifically to the 20 MJ coil. Substantially different losses will be projected as a percent of coil energy for the same conductor operated with different current margins and assumptions of heat transfer in coils of different sizes, as discussed in Section VI.

V. THERMOHYDRAULIC ANALYSIS

Stability. The critical region with respect to stability in this ungraded winding is clearly at the bore of the coil at peak magnetic field. An assessment of the thermal environment for conductor turns in this region during the bipolar pulse shows the rate of heat generation within the conductor strands to be a maximum at the midpoint of the bipolar swing, with a corresponding maximum temperature in the strands as shown in Figure 3. The current-sharing temperature, which is a function of magnetic field, shows a pronounced maximum at the same time, however. Thus, the worst-case situation with respect to stability occurs at peak field immediately subsequent to the pulse when conductor strands rest at 4.5 K and residual bubbles from the AC losses have maximum interference with helium replenishment for stabilization. If all of the losses were to result in the displacement of liquid helium, a gas fraction of 36.1% would be present after the pulse. Since the gas velocity from the conductor is expected to be faster than the liquid velocity, the liquid displacement is expected to be ~20% or less. Thus, the thermal environment just after the pulse is not excessively disturbed by the losses that occur, and a recovery analysis can be pursued in the standard fashion. (It is interesting to note that the 540 kiloJoule coil[5], which was designed for a 50% gas fraction after pulsing, was normalized only after driving it beyond I_c at a current density far in excess of cryostable limits.)

Figure 4 shows the projected curve for heat removal for the 20 MJ strands, including the effects of the thin polyamide-imide insulation. The heat generation curve is almost entirely below the heat removal curve, indicating nearly unconditional recovery of the conductor strands. Very rapid propagation towards the center of the normal region from the cold ends is projected, producing a very nearly uniform and rapid cooling of the conductor throughout the normalized length. The conductor is thus conservatively cryostable. Experiments thus far on heat transfer with the thin polyamide-imide insulation on strand and subcables indicate that the predicted recovery will be achieved[2].

Protection. During the bipolar pulse, and possibly for reasons of control before and after the pulse, large inductive voltages are experienced across the coil terminals. If it is desired that protective mechanisms be triggered in the event of quench, then the discrimination of low resistive voltages amongst large inductive potentials may be required. A protection scheme has been devised to handle this problem, as described in a companion paper[8].

VI. AFFECT OF HEAT TRANSFER AND COIL SIZE ON % LOSS

The losses reported in Section IV are for the 20 MJ coil, conservatively designed as described in this paper. Since increased heat transfer would allow a reduction in stabilizer volume, the loss depends strongly upon the expected heat transfer. In particular, for the 20 MJ strand where substantial margin in I_{op} relative to I_c has been allowed, the number of strands in the cable and the losses can be reduced in inverse proportion to the surface heat transfer. In the first three rows of Table 3, the conductor for the 20 MJ coil is shown in comparison with 50 kiloAmpere conductors using fewer strands identical to those of the 20 MJ design in inverse proportion to the surface heat transfer. Heat transfers of (1) 0.53 Watts/cm^2, the value achieved in tests of Omega-insulated single prototype strands[2], and (2) 0.36 Watts/cm^2, a reasonable but more optimistic projection of achievable heat transfer from the full cable, result in losses of <0.22% and <0.26% of 20 MJ, respectively. If the same conductor is used in a larger diameter coil, for the same peak field the winding thickness becomes a smaller fraction of the coil diameter, a lower % of conductor volume is therefore utilized, and the loss is reduced as a percentage of coil-stored energy. A <0.1% loss is projected, for example, for a 100 MJ coil of a 50 kiloAmpere conductor using 174 20-MJ strands in a -7.9 T to +7.9 T ramped field change in 1.8 seconds as shown in the last row of the Table.

ACKNOWLEDGEMENTS

The authors thank Dr. B. Turck and Dr. G. R. Wagner for helpful discussion of AC losses.

REFERENCES

1. S. K. Singh et.al., "Design of a Superconducting 20 MJ Induction Heating Coil," This Proceedings and Final Report, Los Alamos Scientific Laboratory Contract No. 4-XP9-3459H-1.
2. J. J. Wollan et.al., "Evaluation of a Cryostable, Low-Loss Conductor for Pulsed Field Applications," This Proceedings.
3. S. T. Wang, S. H. Kim, W. F. Praeg, and C. I. Trieger, Proc. of the Seventh Symposium on Engineering Problems of Fusion Research, Knoxville, Tennessee, October 1977, p. 327.
4. M. S. Walker, W. J. Carr, J. H. Murphy, IEEE Trans. MAG 11, p. 1475 (1975).
5. C. J. Mole et.al., Advances in Cryogenic Engineering, 24, p. 57, K. D. Timmerhaus, Editor, Plenum Press (1978).
6. IGC Final Report #1076-3, Los Alamos Scientific Laboratory Contract L66-27851-2.
7. J. J. Wollan, J. D. Rogers, B. A. Zeitlin, M. S. Walker, and T. A. DeWinter, IEEE Trans., MAG 15, p. 816, and test results to be published.
8. M. J. Hennessy, A. W. Heintz, P. W. Eckels, "Quench Detector for Large Pulsed Coils and Quench Analysis for the LASL 20 MJ Coil," This Proceedings.
9. B. Turck, Los Alamos Report #LA-UR-79-411, "Coupling Losses in Various Outer Normal Layers Surrounding the Filament Bundle of a Superconducting Composite, to be published.
10. Syhthesized from existing expressions for this geometry. This is the loss in the copper.
11. J. H. Murphy and M. S. Walker Advanced in Cryogenic Engineering, 24, p. 406 (1978).
12. W. A. Fietz, IEEE Trans. MAG 13, p. 807 (1977).
13. R. Hancox, Proc. of the IEE, Control and Science, 113, p. 1221 (1966).
14. B. Turck, IEEE Trans., MAG 13, p. 548 (1977).

TABLE 1 - 20 MJ CONDUCTOR DESIGN SUMMARY

Operating Characteristics	
Operating Current, I_{op}	50,000 Amperes
I_{op}/I_c at 4.5 K, 7.5 T, 5 x 10^{-11} Ωcm	0.71
J_{op}, Circumscribed Conductor Area	2,615 Amps/cm^2
Fully-Normal Heat Transfer (from 2/3 of Strand Surface)	0.26 Watts/cm^2
Overall Cable Description	
Conductor Length in Coil	677 meters
Cable Dimensions as Wound	1.532 cm x 12.480 cm
Number of Subcables, N	36
Mandrel Core Material	Nitronic 40
Mandrel Size with Insulation	0.257 cm x 11.210 cm
Cable Pitch Angle, Ø	+18 Degrees
Subcable Description	
Number of Nb-Ti Strands, n	6
Subcable Diameter	0.6374 cm
Insulated Core Strand D	0.2238
Pitch Length and Sense	4.670 cm (plus angle)
Core Strand Material	304 Stainless Steel
Insulation on Core Strands	Polyester Amide-Imide (Omega)
Core Strand Insulation Thickness	0.0025 cm
Strand Description	
Metallic Radius, r_s	1.020 mm
Insulation Type	Polyester Amide-Imide (Omega)
Insulation Thickness	0.014 mm
Cu and Filament Core Region, r_f	0.600 mm
Cu-Ni Fin Thickness, t_F	0.064 mm
Copper Outer Shell Thickness, Δr	0.104 mm
Cu-Ni Ring Outer Radius r_c	0.660 mm
Strand Twist, L_s	7.72 mm
Cu Outer Area	1.825 mm^2 (56%)
Cu Core Area	0.633 mm^2 (20%)
Cu Total Area	2.458 mm^2 (76%)
90 Cu-10 Ni Area	0.335 mm^2 (10%)
Nb-Ti Area	0.476 mm^2 (14%)
Metal Area Within r_s	3.269 mm^2 (100%)
Filament Size, d	22.1 μm
# of Filaments, N_f	1,356
RRR Cu Between Filaments	90, 273 K to 4.2 K
RRR Cu Elsewhere	125, 273 K to 4.2 K
ρ_r, Cu-Ni	17 x 10^{-8} Ωm
Helium within Conductor Envelope	43% of Volume

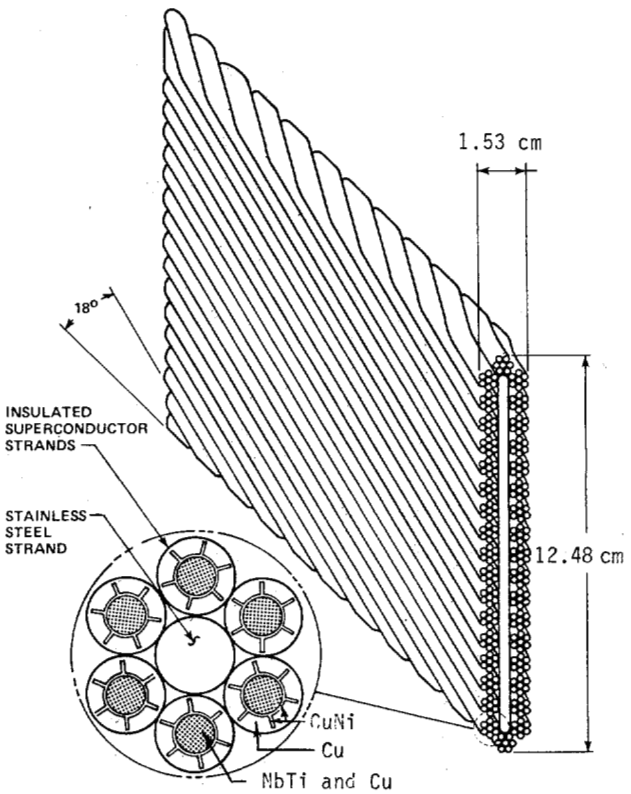

FIGURE 1 20 MJ SUPERCONDUCTING CABLE

TABLE 2 - SUMMARY OF CONTRIBUTIONS TO THE TOTAL AC LOSS FOR ONE SECOND BIPOLAR OPERATION OF THE 20 MJ COIL

Loss Type	Ref. #	Equation	Loss For Coil Alone, % of 20 MJ	Loss As Part of Stack, % of 20 MJ
Transverse Field Strand Losses				
Coupling	(9)	$\frac{P_c}{V_{strand}} = \left(\frac{B_\perp L_s r_f}{2\pi r_s}\right)^2 \left[\frac{1}{\rho_\perp} + \frac{\pi^2}{\rho_r}^{small} + \frac{}{\rho_{Cu\ Outer}}^{small}\right]$, $\rho_\perp = \left(\frac{1+\lambda}{1-\lambda}\right)\rho_{Cu\ Core}$	0.11	.15
Eddy Current	(10)	$\frac{P_e}{V_{strand}} = \frac{\dot{B}_\perp^2}{4\,\rho_{Cu\ Outer}}\left[\frac{r_s^4 - (r_s-\Delta r)^4}{r_s^2\ \text{Shell}} + 6\ \text{Sectors}\left(\frac{r_e^2}{r_s^2}\right)_{small}\right]$	0.07	.08
Hysteresis	(11)	$\frac{P_{ht}}{V_{strand}} = \frac{2\lambda j_c d\,\lvert\dot{B}\rvert}{3\pi} g\left(\frac{I_{op}}{I_c}\right)$	0.04	.05
Transverse Field Strap Loss	(12)	$\frac{P_{ss}}{V_{ss}} = \frac{\dot{B}^2 r_{ss}^2 V_{strand}}{4\,\rho_{ss}\,V_{ss}} + \frac{\dot{B}_{11}^2(t)^2\,V_{strap}}{12\,\rho_{ss}\,V_{ss}} + \frac{\dot{B}^2(w)^2\,V_{strap}}{12\,\rho_{ss}\,V_{ss}}$	0.01	.00
Self-Field Hysteresis Loss	(13)	$\frac{Q_{sf}}{V_{strand}} = \frac{\mu_o I_{op}^2}{4\pi A_{strand}}\left[\frac{(2-F)F+2(1-F)\ln(1-F)}{F^2}\right]$, $F = \frac{I_{op}}{I_c}$	<0.06	<.06
Parallel Field Fully-Coupled Hysteresis Loss	(14)	$\frac{Q_{hp}}{V_{strand}} = \underbrace{\left[\frac{\pi^2 (r_f)^4}{6\,\mu_o\, r_s^2\, L_s^2}\right]}_{K}\left[\frac{(2\,B_{11\,max})^3\,B_c}{(2\,B_{11\,max}+B_c)^2}\right]$, $2\,B_{11\,max} < B_c$	0.02	.03
		$\frac{Q_{hp}}{V_{strand}} = \frac{K\,(2\,B_{11\,max})^3}{4\,B_c}$, $B_c < 2\,B_{11\,max} < 2\,B_c$		
		$\frac{Q_{hp}}{V_{strand}} = 6\,K\,B_c\,(2\,B_{11\,max} - 5/3\,B_c)$, $2\,B_{11\,max} > 2\,B_c$		
		$B_c = \frac{\mu_o \lambda \bar{J}_c L_s}{4\pi}$, Parallel Filament Loss In P_{ht}/V		
Total Loss		Sum of Individual Losses	<0.31	<.37

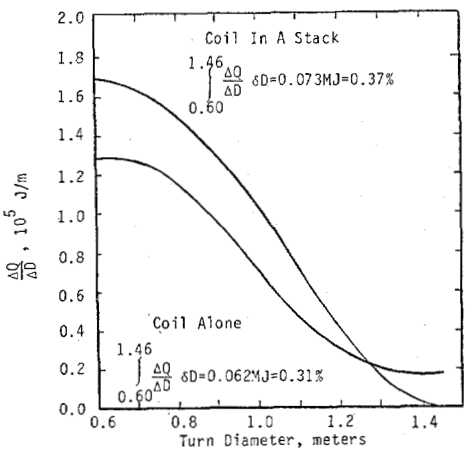

Figure 2 - Maximum AC Loss and Loss Distribution for a One Second Cosinusoidal Bipolar Pulse of the 20 MJ Coil.

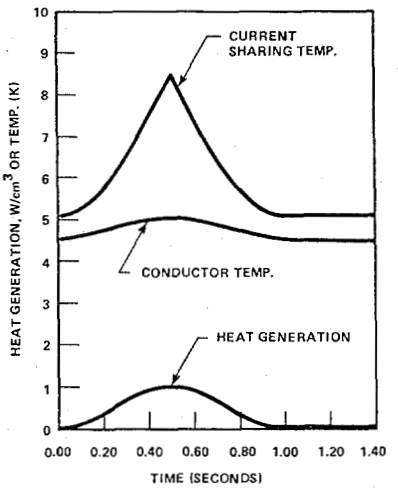

Figure 3 - Conductor Behavior during a Bipolar Pulse

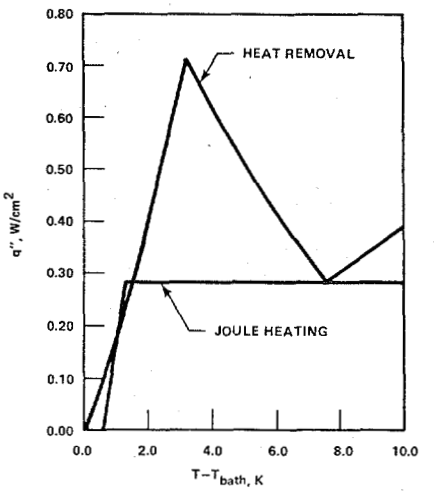

Figure 4 - 20 MJ Conductor Stability

TABLE 3 - AFFECT OF HEAT TRANSFER AND COIL SIZE ON PERCENT LOSS IN 50 KILOAMPERE CONDUCTORS USING THE 20 MJ STRAND DESIGN$^\Delta$

B_{max}, Coil (Tesla)	Heat Transfer (Watts/cm²)	J_{op} 50 kAmp Conductor (Amp/cm²)	Overall Coil J_{op} (Amp/cm²)	A_{sc}/ Strand (mm²)	Strand Dia. (mm)	# of Strands	I_{op}/I_c 4.5K (@ 5×10^{-11} Ωcm)	Bipolar Pulse	AC Loss (% of Coil Energy)
7.5, 20 MJ	0.26, 20 MJ Design	2,615	1,716	0.52	2.0	216	0.71	1 sec ½ cos	< 0.31
7.5, 20 Mj	0.36	3,138	2,059	0.52	2.0	180	0.86	1 sec ½ cos	< 0.26
7.5, 20 MJ	0.53	3,733	2,450	0.52	2.0	150	1.02	1 sec ½ cos	< 0.22
7.9, 100 MJ†	0.36	3,071	2,014†	0.52	2.0	174	1.06	1.8 sec ramp	< 0.10

† Assuming 20 MJ type of construction will be applicable for 100 MJoule coil.
Δ Losses for coils operating alone (as opposed to in a stack).